A&A 454, 473–480 (2006)
DOI: 10.1051/0004-6361:20054776

Astronomy & Astrophysics

Multifractality in a ring of star formation: the case of Arp 220

R. de la Fuente Marcos and C. de la Fuente Marcos

Suffolk University Madrid Campus, C/ Viña 3, 28003 Madrid, Spain
e-mail: raul@galaxy.suffolk.es

Received 26 December 2005 / Accepted 21 March 2006

ABSTRACT

Context. Formation of super star-clusters can be triggered during the final stages of galaxy mergers or galactic interactions, when significant numbers of massive stars are formed out of large gas-cloud systems. Giant cloud complexes show a fractal structure due to turbulence and/or self-gravitation; therefore, super clusters formed out of these complexes are expected to show a multifractal spectrum.
Aims. Here we investigate the projected spatial distribution of young massive clusters in the ultraluminous infrared galaxy Arp 220 and its underlying fractal geometry.
Methods. The projected radial distribution of super clusters is dominated by a prominent ring of star formation. Taking the presence of this annulus into account, the fractal spectrum is determined by using the Minkowski-sausage method to compute the Minkowski-Bouligand dimension as a function of the parameter q.
Results. The ring appears to extend from a radial distance of 2.0 to 4.5 kpc. The Arp 220 annulus of star formation could be an outer ring associated with the outer Lindblad resonance/radius of corotation. The average projected fractal dimension in the ring of star formation is found to be 1.7 ± 0.1, which is consistent with values found for non-starburst, star-forming regions in spiral galaxies. However, the fractal dimension appears to be lower in the outer regions of the ring and, for Arp 220, this implies an actual decrease in the fractal dimension over time probably induced by star cluster destruction. This trend is not observed under quiescent star formation.
Conclusions. The projected distribution of super clusters in Arp 220 can be described using an annular model, and it exhibits multifractal behaviour. The properties of its fractal geometry are similar to those found in quiescent star-forming regions in disk galaxies although the average fractal dimension evolves differently over time, decreasing instead of increasing. This result implies that, for the short-term evolution of super cluster populations, destruction may be far more important than diffusion-like processes.

Key words. galaxies: starburst – galaxies: star clusters – galaxies: individual Arp 220 – stars: formation – galaxies: interactions – galaxies: peculiar

1. Introduction

Halton Arp included the irregular galaxy IC 4553 (UGC 9913 = Zw 136.017 = MGC +04-37-005 = IRAS 15327+2340 = LEDA 55497) in his *Atlas of Peculiar Galaxies* (Arp 1966a,b) as entry 220 under the section "galaxies with adjacent loops". The low-resolution, optical image of this object shows a double structure with faint extended loops or tails. The bilobal structure is caused by a dust lane that bisects the object. These peculiar features suggest that Arp 220 may be the remnant of a recent merger of two galaxies. Early studies pointed out the possible presence of a highly peculiar double nucleus (Nilson 1973; Stocke et al. 1978), while observations in radio and the infrared suggested that the object was either a starburst galaxy (Weedman et al. 1981; Baan et al. 1982; Joseph et al. 1984; Rieke et al. 1985) or Seyfert galaxy (Soifer et al. 1984; Norris et al. 1984; Norris 1985), which radiated virtually all of its energy in the far-infrared continuum (Soifer et al. 1984). Joy et al. (1986) showed that the far-infrared and optical structures of Arp 220 were consistent with the outcome of a galactic collision and subsequent merger. The merger of two spiral galaxies scenario was also proposed by Joseph & Wright (1985) and Sanders et al. (1988). Graham et al. (1990) found a double nucleus in Arp 220 with a separation of 0.95 arcsec, both of them showing barlike morphology.

The Hubble Space Telescope (HST) revealed the presence of super star-clusters (Shaya et al. 1994) in Arp 220. Near-Infrared Camera and Multiobject Spectrometer (NICMOS) imaging with the HST provided a clear picture of the central region of Arp 220 with the two nuclei and a number of luminous super star-clusters (Scoville et al. 1998). The twin nuclei were studied further by Sakamoto et al. (1999) and Soifer et al. (1999). Faint tidal tails and distortions in HI emission in the outer parts of Arp 220 were identified by Hibbard et al. (2000). Shioya et al. (2001a) studied super star-clusters within 2.5 kpc from the centre of Arp 220 finding an age range of 10−100 Myr for a sample of 6 objects. Chandra X-rays observations of Arp 220 showed a source of hard, X-ray emission in the nuclear regions of Arp 220 (Clements et al. 2002). Using mid-infrared spectra and X-ray observations, Spoon et al. (2004) pointed out that one of the nuclei may host the most highly obscured Active Galactic Nucleus (AGN) known. Using the Advanced Camera for Surveys (ACS) of the HST through its High Resolution Channel (HRC), Wilson et al. (2006) have identified 206 probable clusters in Arp 220 with two different age groups.

Ultraluminous infrared galaxies are the most luminous objects in the local universe with bolometric luminosities $> 10^{12}\ L_{\odot}$. Assuming $H_0 = 72 \pm 8$ km s^{-1} Mpc^{-1} (Freedman et al. 2001) and $\Omega_0 = 1$ with a recessional velocity to the Galactic standard of rest of 5531 km s^{-1} (de Vaucouleurs et al. 1991), Arp 220 is located at a distance of 77 Mpc in the constellation of Serpens. At this distance, Arp 220 is the closest representative of the ultraluminous infrared galaxy class. More than 95% of its

total bolometric luminosity is emitted at infrared/submillimetre wavelengths (1.3×10^{12} $L_{\odot}$, Soifer et al. 1984; Sanders et al. 1988, 2003). It also exhibits a wide variety of molecular lines originating in an extremely dense central condensation of dusty gas, and it is regarded as the prototypical OH megamaser galaxy. Arp 220 is now considered an advanced merger system involving two relatively large, gas-rich spiral galaxies with two nuclei currently separated by about 350 pc. The primary nucleus (located west) shows a crescent shape, concave to the south, and the secondary nucleus (southeast) is bifurcated by a dust lane (Scoville et al. 1998). As a result of the merging process, a starburst is taking place in the central regions of the system. Starburst models (Shioya et al. 2001b) of the nuclear starburst in Arp 220 indicate a local star formation rate of 270 $M_{\odot}$ yr^{-1} that is, probably, the largest in the local universe (Wilson et al. 2006). Sanders et al. (2003) give a value of 240 $M_{\odot}$ yr^{-1} for the total current star formation rate.

Direct (non-grazing) galaxy collisions are accompanied by collisions between giant molecular clouds located in the few kiloparsec-wide, central regions of the involved galaxies. Collisions between clouds may trigger a gravitational instability in the bulk of the colliding giant molecular clouds that can result in the formation of massive clusters. In non-starburst star-forming regions, star clusters form out of collapsing cloud clumps in molecular clouds (Tilley & Pudritz 2004). Collapse is triggered by turbulent fragmentation of clouds and their clumps (MacLow & Klessen 2004). Formation of complexes of young massive clusters or super clusters could be driven by the same processes operating in quiescent star-forming regions (Larsen & Richtler 2000); the only difference is in the extreme conditions (high pressure and very large amounts of gas available in a relatively small region) present during violent starburst episodes. On the other hand, interstellar gas, giant molecular clouds, and stars in galaxies are observed to have a fractal structure ranging from subparsec to several kiloparsec scales (see Elmegreen & Elmegreen 2001, and references therein). Fractals are geometric objects with dimensionalities that are not integers. They play a fundamental role in the dynamics of chaotic systems (Mandelbrot 1982, 1985). It is usually assumed that the fractal dimension of interstellar clouds is 2.3 (Elmegreen & Falgarone 1996), although other authors suggest values closer to 2.7. In particular, Feitzinger & Galinski (1987) found an average value of 1.7 for the projected fractal dimension of the distribution of star-forming sites (HII regions) in a sample of 19 spiral galaxies. Recently, Sánchez et al. (2005) found a value of about 2.6 for the Orion A star-forming complex. De la Fuente Marcos and de la Fuente Marcos (2006) found an average value of the fractal dimension of 1.7 ± 0.2 for the spatial distribution of young open clusters (age < 40 Myr) in the Solar Neighbourhood.

If quiescent and starburst-driven star formation can both be explained by the same mechanisms, it is natural to expect that the spatial distribution of young massive clusters should follow a fractal pattern, too, and that its fractal dimension should perhaps be close to the values found in non-starburst star-forming regions. Here we show evidence for such a fractal pattern in a sample of super star-clusters in the ultraluminous infrared galaxy Arp 220 taken from a survey carried out by Wilson et al. (2006). We also estimate the value of the fractal dimension of this pattern. This paper is organised as follows. In Sect. 2 we briefly present the data analysed. The projected spatial distribution of young massive clusters is studied in Sect. 3. The multifractal analysis method is described in Sect. 4. In Sect. 5 we present the multifractal properties of the projected spatial distribution. In Sect. 6 we discuss our results. Finally, in Sect. 7 we summarise our conclusions.

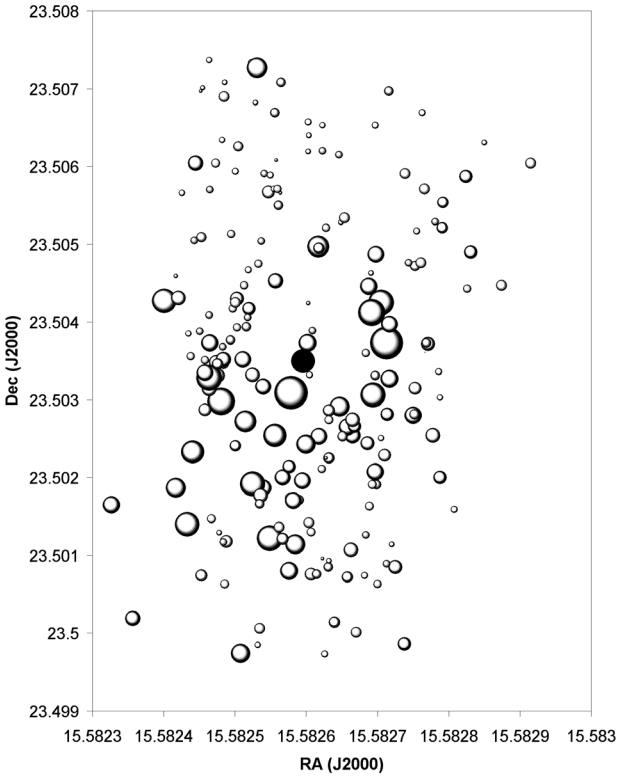

Fig. 1. Positions of the objects in the sample of 206 cluster candidates compiled by Wilson et al. (2006). The radius of each point is proportional to the value of the $V-I$ colour index of the associated object. The black circle represents the position of the centroid of the entire population at α(J2000) = $15^{\rm h}.5826$, δ(J2000) = $23^{\circ}.5035$.

2. Data

In order to evaluate the fractal dimension of young massive star clusters in Arp 220, we use the sample compiled by Wilson et al. (2006). Their Table 2 includes 206 candidate objects with accurate positions for all of them. The set can be considered as an age-limited, volume-limited cluster sample in Arp 220. All the objects are located within a 7 kpc circle around Arp 220 double nucleus (see Fig. 6, Wilson et al. 2006). Figure 1 shows the location of all the objects in Table 2 of Wilson et al. (2006). The radius of each point in Fig. 1 is proportional to the value of the colour index $V-I$. The centroid of the entire population is shown as a black circle (α(J2000) = $15^{\rm h}.5826$, δ(J2000) = $23^{\circ}.5035$, or in actual pixels $X = 562$, $Y = 598$) and coincides approximately with the position of the solid cross in Fig. 6 ($X \sim 614$, $Y \sim 623$, Wilson et al. 2006), which is the galaxy centre quoted in Scoville et al. (1998).

These super star-clusters appear to fall into two different age groups: a younger population with an age < 10 Myr and an intermediate age population of about 300 Myr. A small number are possibly old globular clusters. Although Wilson et al. (2006) only give ages for a subsample of 14 (out of 206) clusters, we have observed that the $V-I$ colour index of clusters in the younger age group shows a strong trend toward >0.8, with clusters in the intermediate age group usually <0.8. If this trend can be considered as a rough age indicator and taking into account that the point radii in Fig. 1 are proportional to the value of the $V-I$ colour index, we may conclude that the younger

age group members are significantly closer to the galaxy centre. The centroid of the subsample with $V - I \leq 0.8$ (83 objects) is located at α(J2000) = 15$^{\rm h}$.5826, δ(J2000) = 23°.5042, or in actual pixels $X = 465$, $Y = 599$. The centroid of the subsample with $V - I > 0.8$ is located at α(J2000) = 15$^{\rm h}$.5826, δ(J2000) = 23°.5030, or in actual pixels $X = 623$, $Y = 552$. This appears to suggest that the majority of objects in the studied sample are, in fact, part of the younger age group and that the merging process is in its final stages.

Many of the clusters in Wilson et al. (2006) appear to have masses in the range 10^5–10^6 $M_\odot$ and up to 10^7 $M_\odot$, which are even larger than those of the most massive clusters observed in the Antennae (Whitmore et al. 1999). These numbers make them clear proto-globular cluster candidates. Wilson et al. (2006) indicate that the members of the younger age group are more centrally concentrated (i.e. their relative distances are smaller) than the ones in the intermediate age group, which tend to be found preferentially towards the outskirts of the studied region (i.e. their relative distances are larger). The centre of the young group is located 1 kpc east of the double nucleus and the average radius is 1.6 kpc. The intermediate age group is centred about 3 kpc north of the double nucleus with an average radius of 3 kpc. The centroids of the two populations are not located at the centre of the galaxy, and they do not appear to be specifically associated to any of the two nuclei. The inter-nuclei distance is only about 350 pc, much smaller than the characteristic distances quoted above. Wilson et al. (2006) indicate that the super star-cluster sample is not complete, with probable missing intermediate age clusters at large radii and also in the inner regions of the galaxy due to the high value of the interstellar extinction there. The actual degree of incompleteness can affect our subsequent results, so it will be discussed in detail below.

3. The ring of fire: cluster radial distribution

To perform a consistent analysis of the fractallity of the spatial distribution of young massive clusters in Arp 220, we first examine the cumulative projected radial distance distribution: $N(r < d) \propto r^{\beta}$, where $N(r < d)$ is the cumulative number of objects with distance shorter than d, and β is the exponent of the (assumed) power-law distribution. In principle, $N(r < d)$ is also an implicit function of the time as the sample in Wilson et al. (2006) includes objects of, at least, two different age groups that show systematic trends in their radial distribution. However, the actual functional form of this time dependence cannot be obtained easily from the available data, so it will be ignored here. If we represent the cumulative distribution function for distances, we observe an unusual behaviour (see Fig. 2): saturation at small and large distances from the centre. The error bars in N have been estimated from a Poisson distribution with mean error $\sqrt{N}$. A least-squares linear fit to the double logarithmic plot gives:

$$\log(N(r < d)) = 0.92(\pm 0.15) + 1.8(\pm 0.2) \log(r(\mathrm{kpc})). \quad (1)$$

Therefore the exponent of the power-law fit is $\beta = 1.8 \pm 0.2$. The product-moment correlation coefficient, or Pearson's r is 0.95. On the other hand, for a projected distribution of points, the radial number density can be written as:

$$\sigma = \frac{N(r < d)}{\pi\, r^2}. \quad (2)$$

Besides, the radial number density may also be described by a power law:

$$\sigma \propto r^{-\alpha}. \quad (3)$$

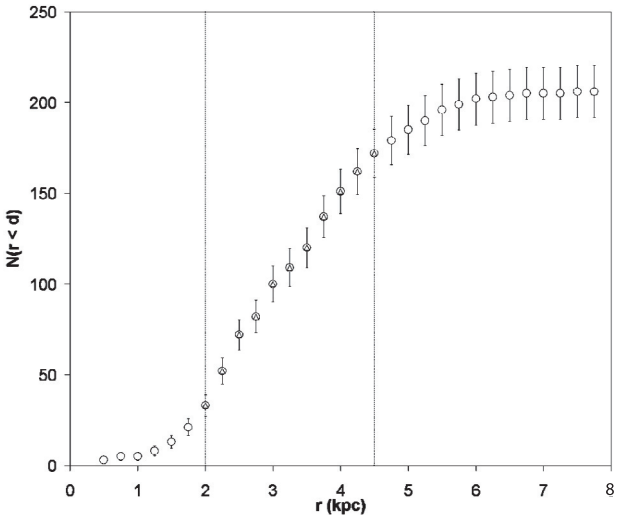

Fig. 2. Cumulative projected radial distance distribution for the sample of 206 cluster candidates in Wilson et al. (2006). The adopted centre coincides with the black circle displayed in Fig. 1.

Taking both equations into account, we can also write

$$N(r < d) \propto r^{2-\alpha}, \quad (4)$$

therefore, $\beta = 2 - \alpha$. In our case, $\alpha = 0.2 \pm 0.2$, which is compatible with constant density within the error limits.

In any case, the radial distribution of super star-clusters in Arp 220 reveals the presence of a prominent ring or annulus of star formation located at an average distance of 3.3 kpc from the centroid of the star cluster population. The inner edge of this ring of star formation appears to be located at about 2 kpc from the centroid, well beyond the nuclear zone, and it seems to coincide with the edge of the first annulus considered in the radial distribution of clusters in Arp 220 by Wilson et al. (2006). The outer rim of the annulus is found at about 4.5 kpc from the centroid that is also the radial distance considered in Wilson et al. (2006) for the separation between their second and third annuli (see Fig. 2).

Although the prominence of the ring is rather clear, it should be taken with some caution because the saturation (flat slope) observed for $r < 1.5$ kpc and $r > 6$ kpc could be the result of incompleteness, as Wilson et al. (2006) state in their paper: some missing clusters are expected in the intermediate age group at both small and large radii. In this case, the observed behaviour could be interpreted as a sign of instrumental truncation, a systematic error induced by the data reduction procedure. If true, the degree of incompleteness could be significant. The actual importance of this problem appears to be, however, small as our subsequent multifractal analysis suggests. Although one may still argue that the distribution in Fig. 2 is probably severely distorted by the double nuclei and extinction, this interpretation is not favoured by Wilson et al. (2006). They only consider the effect of the extinction important for the central regions. The central region of Arp 220 is shrouded in large amounts of dust, which may explain the almost circular region devoid of star clusters observed in Fig. 1, i.e. the saturation observed at small radii in Fig. 2.

Almost certainly, the radial distance distribution curve is shallow in the inner parts because of extinction, as Wilson et al. (2006) point out that there is large extinction there (>1000 mag in V). The flat outer part is probably because the edge of the galaxy is reached; therefore, it is the result of the overall disk

radial profile. Although we do not have any explicit time dependence in the above distribution, there is an implicit one linked to the fact that the younger population is most likely found at small radial distances and the intermediate age population is located, on average, at larger radii. If star formation is mostly over at large radial distances in Arp 220, then the observed saturation perhaps has to be connected to gas depletion (or incompleteness, but that is partially ruled out in Wilson et al. 2006). Conversely, at small radial distances a larger fraction of young clusters is observed, and if they are being formed now, it is because there is still gas available. Older clusters may still remain undiscovered due to the high value of the extinction in the central regions of Arp 220. We did not attempt to include any explicit time dependence in our simplified modelling because there is no extensive and reliable information on cluster ages in the original Wilson et al. (2006) paper.

If we focus our attention on the ring of star formation, we observe that it includes 139 candidate star clusters or about 67% of the sample. A least-squares linear fit to the cumulative projected radial distance distribution within the ring region gives:

$$N(r < d) = 54.62\ r(\mathrm{kpc}) - 69.33, \tag{5}$$

with a correlation coefficient of 0.9987. A logarithmic approach gives an almost equal correlation coefficient (0.9974):

$$N(r < d) = 391.62\ \log(r(\mathrm{kpc})) - 86.92. \tag{6}$$

Although thicker, the ring identified in Arp 220 appears to be similar to other rings of star formation found in spiral galaxies. The Andromeda galaxy (M 31) hosts a bright and prominent ring of star formation at ∼10 kpc from the centre (Habing et al. 1984; Rice 1993; Gordon et al. 2006). As the clusters are distributed in a ring, calculating the fractal dimension for the whole set has no physical meaning, so a more careful approach has to be implemented.

4. Multifractal analysis

A variety of objects in astrophysics are described as fractals but none of them are actual fractals, as their fractal features disappear if they are viewed on sufficiently small scales. Nevertheless, they appear very much like fractals over certain ranges of scale, and on such scales they can be described using fractal techniques. A fractal point distribution can be described in terms of its fractal dimension. Many apparently different definitions of dimensionality are currently used in nonlinear dynamics. In the present work we adopt the working definition and procedure described by Yadav et al. (2005). These authors have carried out a multifractal analysis of the galaxy distribution in the Sloan Digital Sky Survey Data Release One to conclude that the galaxy distribution is homogeneous on scales larger than $60-70\ h^{-1}$ Mpc.

Let us consider a projected, finite distribution of N super star-clusters. Labelling the objects from 1 to N and using $\boldsymbol{x}_i$ and $\boldsymbol{x}_j$ to denote the galactocentric coordinates (referring to the geometric centre of the projected distribution in Arp 220, the black circle in Fig. 1) of the ith and jth super star-clusters, respectively, then the number of other clusters within a circle of radius r (from now on we use r as the radius of the working circle instead of radial distance as in the previous section) centred on the ith super star-cluster is given by the expression

$$n_i(r) = \sum_{j=1, j\neq i}^{N} \Theta(r - |\boldsymbol{x}_i - \boldsymbol{x}_j|), \tag{7}$$

where $\Theta(x)$ is the Heaviside function defined such that $\Theta(x) = 0$ for $x < 0$ and $\Theta(x) = 1$ for $x \geq 0$. This summation is over the whole set of super star-clusters with coordinates $\boldsymbol{x}_j$, $j \neq i$. If we choose M different clusters as centres to evaluate the previous expression and calculate the average

$$C_2(r) = \frac{1}{M(N-1)} \sum_{i=1}^{M} n_i(r), \tag{8}$$

we obtain the probability of finding a young massive star cluster within a circle of radius r centred on another cluster. This summation is over a subset of M objects, taken as centres, with coordinates $\boldsymbol{x}_i$. By taking only M clusters as centres, we allow for the effect of the finiteness of the sample. As r goes to zero, $C_2(r)$ can be described as a power-law function of the radius of the circle, $C_2(r) = k\ r^{D_2}$, and then the exponent D_2 can be identified with the fractal dimension of the projected young massive star cluster sample distribution. It is necessarily ≤ 2 for an embedding space of dimension two (Falconer 1990; Schroeder 1991); when D_2 is different from two, the distribution is fractal. For computational purposes it is more convenient to use the form: $\log(C_2(r)) = K + D_2\ \log(r)$, where K is a constant. Here, D_2 is called the two-point correlation dimension (or correlation dimension for short).

Unfortunately, the two-point correlation is not enough to provide a statistically complete description of the properties of the distribution of super star-clusters; the full statistical quantification of a fractal distribution cannot be based on one scaling index. In order to provide an exhaustive description of the distribution of young massive star clusters in Arp 220, higher order correlations have to be studied. The use of the $(q-1)$th moment of $n_i(r)$ enables the generalization of the two-point correlation dimension as the Minkowski-Bouligand dimension (Minkowski 1900; Bouligand 1928a,b, 1929), D_q given by

$$D_q = \lim_{r\to 0} \frac{1}{q-1} \frac{\log C_q(r)}{\log r}, \tag{9}$$

and

$$D_1 = \lim_{q\to 1} D_q, \tag{10}$$

where

$$C_q(r) = \frac{1}{M(N-1)} \sum_{i=1}^{M} (n_i(r))^{q-1}, \tag{11}$$

implicitly assuming $C_q(r) = k\ r^{(q-1)D_q}$. The Minkowski-Bouligand dimension is also called the generalized fractal dimension (see, e.g., Grassberger 1983; Grassberger & Procaccia 1983). In general, the scaling behaviour of $C_q(r)$ depends on the length-scale. A monofractal is characterised by a single value of the Minkowski-Bouligand dimension, independent of q. Variations of the Minkowski-Bouligand dimension with q are typical of multifractal distributions. In multifractals, the whole spectrum of singularity exponents is required to accurately describe their geometrical properties (Falconer 1990).

In our case, the positive values of q place more importance on the regions of Arp 220 where the number density of young massive star clusters (star-forming complexes) is higher, whereas the negative values of q favour the contribution of underdense zones. The Minkowski-Bouligand dimension characterises the scaling of relatively empty regions for $q < 0$ and describes the scaling behaviour of the young massive star cluster distribution within star-forming complexes for $q > 0$. A

fractal dimension of 3 indicates spatial randomness in a three-dimensional space, a value of 2 indicates spatial randomness in a two-dimensional space. A fractal dimension of 0 would mean complete clumping, with all the objects concentrated at a single point. One may argue that the distribution is not fractal because it involves cutoff scales. The inner cutoff can be identified as the smallest intercluster distance, 0.05 kpc, and the outer cutoff is the size of the stellar field studied in Wilson et al. (2006), 7 kpc. Therefore we are actually calculating the effective fractal dimension within these cutoff scales.

5. Multifractality in a ring of fire

Although the limit in Eq. (9) cannot be computed mathematically, it can be estimated statistically. Following the method described above and in order to compute the multifractal spectrum of the point set, we will cover it with overlapping circles of constant radius r (the r-sausage of Minkowski, Minkowski 1900) and retain the points of the original set that lie within the boundary of this covering r-sausage of convex structuring elements (filled circles). Our point set is the distribution of super star-clusters in Arp 220 and r is the radius of the circles used for covering the points.

Using the method outlined above with the statistical approach, we have analysed the sample of young massive star cluster candidates presented in Sect. 2. In Arp 220 the distribution of clusters is concentrated in a ring around the centre of the galaxy. A ring or disk with a hole is not topologically equivalent to a disk. A disk is a simply connected space or domain, and a disk with a hole (annulus or ring) is non-simply connected or multiply connected. Although the region studied in this section is not simply connected, it is possible to rectify this defect by using its universal cover, a simply connected space. In our case, this simply connected space is the circle covering. The presence of a ring structure imposes two different sets of cutoffs. The inner and outer radii of the ring are the structural cutoffs, so we have then the lower cutoff associated to the smallest inter-cluster distance within the studied ring and the upper cutoff defined by the thickness of the ring or the largest inter-cluster distance (physical cutoffs). If the original star cluster distribution follows a two-dimensional fractal pattern but only a ring of this original distribution is used to calculate the fractal dimension, then only the information for length-scales smaller than the thickness of the ring will be recovered. For length-scales larger than the ring thickness, the information on the fractal pattern cannot be recovered due to the presence of the additional structural cutoffs.

For each super star-cluster within the structural cutoffs, we construct a circle of radius r and count all the other super star-clusters enclosed by the circle. The radius changes within the range defined by the smallest inter-cluster distance and the semi-thickness of the ring; super star-clusters with r-circles not fully included in the ring are removed from the analysis. Then we draw the log-log plot of $C_q(r)$ versus r (see Fig. 3), estimate the value of the slope of the graph $\tau(q)$ with a linear regression, and obtain a dimension given by

$$D_q = \frac{\tau(q)}{q-1}, \tag{12}$$

$$D_1 = \lim_{q \to 1} D_q. \tag{13}$$

This method assumes $C_q(r) \propto r^{(q-1)\,D_q}$ as before, although for computational purposes, it is more convenient to use the form

$$\log(C_q(r)) = K + (q-1)\,D_q\,\log(r), \tag{14}$$

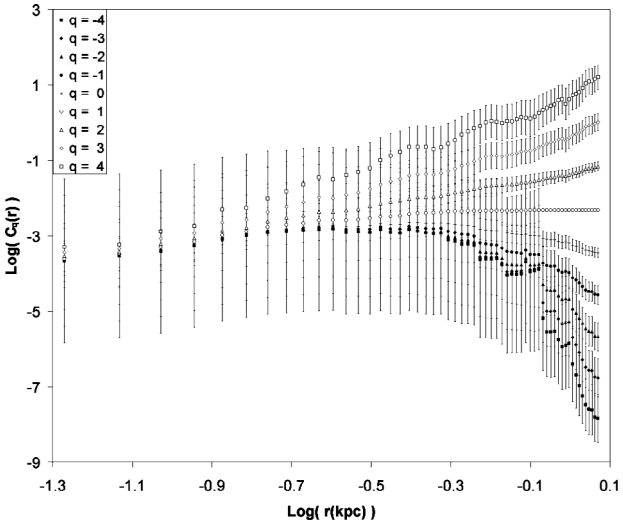

Fig. 3. $C_q(r)$ for all the values of q studied for the sample of 206 young massive star clusters in Arp 220 from Wilson et al. (2006).

where K is a constant. The generalized dimensions given by Eq. (12) provide a spectrum of dimensions. This spectrum of dimensions characterises the multifractal. It can be proved (Paladin & Vulpiani 1987) that the generalized dimensions are monotonically decreasing functions of q. In this first analysis the lower cutoff is about 50 pc and the upper cutoff around 1.2 kpc. When the Minkowski-Bouligand dimension is constant for all q, the multifractal can be described by a single index (monofractal).

For each object we consider a circle of radius r centred on the cluster and counted the number of other clusters to determine $n_i(r)$. The characteristic radius is in the range 0.05−1.17 kpc and the circle is always within the boundaries defined by the sample (if not, the centre is rejected). The values of $n_i(r)$ calculated using different clusters as centres are then averaged to calculate $C_q(r)$ (see Fig. 3). In order to keep the circle within the boundaries of the samples, the number of centres decreases when r increases. In any case, the application of multifractal estimators to actual data must be performed with extreme care. No single estimator can be used with any confidence for a range of q values that probe both low- and high-density regions in the data (Wu et al. 1997). Unfortunately, for our data set this method appears to be robust for all regions with one exception, $q \leq 0$ for $r < 0.4$ kpc. There, the spectrum is not monotonically decreasing with increasing q (see Fig. 4). In fact for that range, it is compatible with a value of zero, within the error limits.

Figure 4 shows the multifractal spectrum of the young massive cluster distribution in Arp 220. For length-scales < 0.4 kpc, the Minkowski-Bouligand dimension for $q \leq 0$ increases slightly with q (which is unphysical). This suggests that some artefacts are present due either to the method used in our analysis or to the cluster sample. The physically meaningful values of the Minkowski-Bouligand dimension within the ring are: $D_2 = 1.754 \pm 0.015$, $D_3 = 1.32 \pm 0.03$, and $D_4 = 1.16 \pm 0.05$ with correlation coefficients larger than 0.9931. These values characterise the multifractallity of ring of star formation in Arp 220. If we consider D_2 as the effective fractal dimension of the data set, the unprojected fractal dimension is $\langle D \rangle = 2.7$. Errors for $q > 0$ are less than 3%, but they could be up to 36% for $q < 0$.

If we repeat the analysis using a set of concentric rings of thickness 1 kpc to check the previous results for consistency we obtain the multifractal spectrum shown in Fig. 5. For the

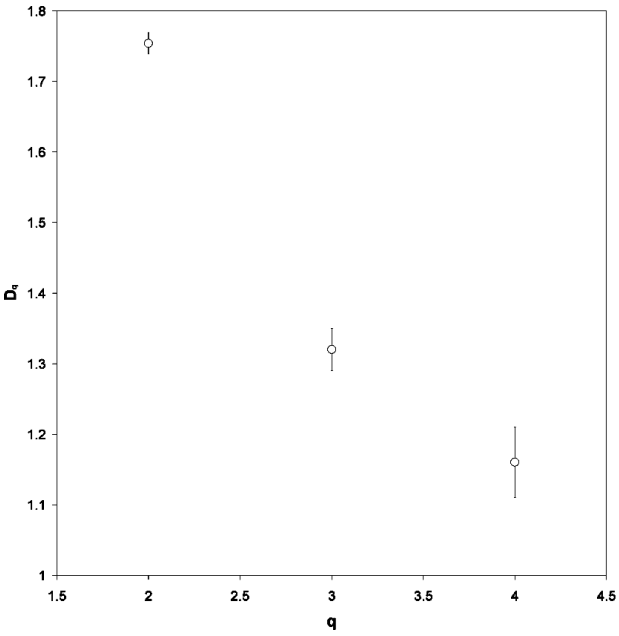

Fig. 4. Spectrum of the Minkowski-Bouligand dimension as a function of q for young massive star clusters in Arp 220.

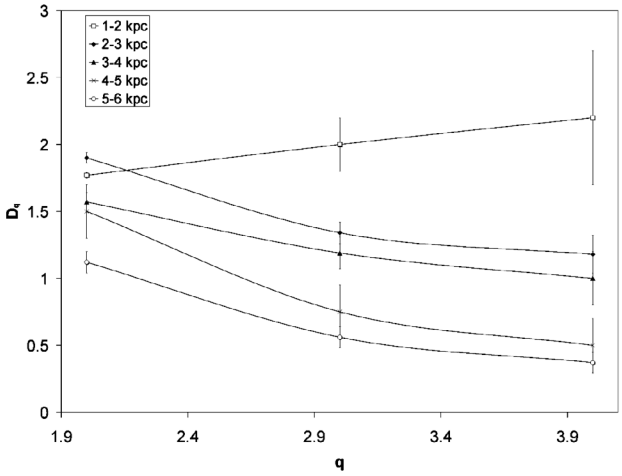

Fig. 5. Annular analysis of the spectrum of the Minkowski-Bouligand dimension as a function of q for young massive star clusters in Arp 220.

central kiloparsec in Fig. 1 it is not possible to calculate any estimate of the fractal dimension. For an annulus of radii 1−2 kpc, the physical cutoffs are 0.15 and 0.23 kpc, and the values of the Minkowski-Bouligand dimension are: $D_2 = 1.77 \pm 0.02$, $D_3 = 2.0 \pm 0.2$, and $D_4 = 2.2 \pm 0.5$ with correlation coefficients larger than 0.99. This result is unphysical as the dimension increases with q although the errors are quite large. For an annulus of radii 2−3 kpc, the physical cutoffs are 0.05 and 0.41 kpc, and the values of the Minkowski-Bouligand dimension are: $D_2 = 1.90 \pm 0.04$, $D_3 = 1.34 \pm 0.08$, and $D_4 = 1.18 \pm 0.14$ with correlation coefficients larger than 0.99. Still inside the ring previously analysed, for an annulus of radii 3−4 kpc the physical cutoffs are 0.17 and 0.43 kpc, and the values of the Minkowski-Bouligand dimension are: $D_2 = 1.57 \pm 0.07$, $D_3 = 1.19 \pm 0.12$, and $D_4 = 1.0 \pm 0.2$ with correlation coefficients larger than 0.97. Within the annulus defined by the range 2−4 kpc the average value of the fractal dimension is $\langle D_2 \rangle = 1.74 \pm 0.11$. For an annulus of radii 4−5 kpc the physical cutoffs are 0.23 and 0.39 kpc, and the values of the Minkowski-Bouligand dimension are: $D_2 = 1.5 \pm 0.2$, $D_3 = 0.7 \pm 0.2$, and $D_4 = 0.5 \pm 0.2$ with correlation coefficients larger than 0.93. Finally, for an annulus of radii 5−6 kpc the physical cutoffs are 0.09 and 0.47 kpc, and the values of the Minkowski-Bouligand dimension are: $D_2 = 1.12 \pm 0.08$, $D_3 = 0.56 \pm 0.08$, and $D_4 = 0.37 \pm 0.08$ with correlation coefficients larger than 0.95.

For the radial distance intervals 0−1 kpc and 4−6 kpc, the values of $C_q(r)$ do not depend on q due to the large inter-cluster distance. This is the result of extinction-induced incompleteness at small radial distance and (very likely) cluster destruction or (less likely) incompleteness at large distance from the centre. The errors associated to D_2 are always less than 3%. On the other hand, the average, effective fractal dimension of concentric annuli in Arp 220 appears to decrease outwards, and there is a systematic variation in the average age of the super star-cluster population with the radial distance, increasing outwards. Therefore, the different values found for the effective fractal dimension of the two age groups strongly suggest that the fractal dimension of super star-clusters in Arp 220 decreases over time (the observed differences cannot be attributed to large errors). If it decreases over time, this can be interpreted as evidence of super star-cluster complexes disintegrating on a relatively short time-scale, although a more detailed discussion will be carried out in the following section. The final value of the fractal dimension of the distribution of young massive star clusters in Arp 220 can be written as 1.7 ± 0.1. Clear signs of self-similarity are found in the multi-annuli analysis (see Fig. 5). The nature of the variation of the fractal dimensions with the length-scale considered suggests that most of the clusters in the Wilson et al. (2006) sample (likely up to 70%) are part of the younger age group.

6. Discussion

Arp 220 is the brightest object in the local universe. The central regions of this peculiar galaxy host a collision between two very similar spiral galaxies. The collision has provided the triggering mechanism for a burst of star formation. The remnant cores of the two colliding galaxies are located about 350 pc apart and orbit each other. That one of the cores is crescent moon-shaped suggests that this core has an associated disk of dust about 80 pc wide and may be hiding a supermassive black hole. Numerical simulations of collisions between counter-rotating, gas-rich disk galaxies of similar mass (Hearn 2002) with the impact velocity roughly parallel to the galactic spin axes (head-on collision) show that the ram pressure and large-scale gravitational contraction that occur in the gaseous components of a colliding system can produce extensive regions of shock-heated gas, as well as many of the morphological structures observed in Arp 220.

Binary supermassive black holes are expected to form following galactic mergers. Begelman et al. (1980) pointed out that the central black holes of two galaxies will coalesce in the course of a galactic merger. During the late stages of the merger, the two supermassive black holes move through the stellar component and the compressed interstellar gas with a similar velocity to the initial relative motion between the two galaxies. Eventually, the increasing dynamical friction will lead the black holes to the newly-formed galactic centre. During this process, the two black holes will end forming a binary system (Makino 1997), a supermassive binary black hole. It is very likely that Arp 220 is currently undergoing this phase. Using numerical simulations, Hemsendorf et al. (2002) have shown that the binary is hardened by three-body encounters with single stars. The final result is a very eccentric (eccentricity 0.7) supermassive binary black hole

with a semi-major axis of 0.6 pc. In a typical model, the initial distance between the black holes is 355.39 pc. This separation is similar to the one found in Arp 220's double nuclei.

Although the distribution of super star-clusters does not provide significant information on the dynamics of the nuclear regions in Arp 220, it clearly reveals the morphology of the outer regions. The most prominent structure is a thick ring or annulus of star formation found between 2.0 and 4.5 kpc from the nuclear regions. Most of the super star-clusters included in this research appear to be part of this structure. The outer rim of the galactic disk formed during the merger of Arp 220 could be located at about 6 kpc from the centre. Galactic rings could be the result of internal resonances or galactic interactions. Buta (1986) has shown that internal resonances can cause three different types of rings: nuclear, inner, and outer. A nuclear ring in Arp 220 was proposed by Scoville et al. (1998) with a circumnuclear envelope at radii 700−2300 pc. The Arp 220 ring found in this research is clearly not a nuclear or inner ring usually connected with the presence of a bar. The Arp 220 ring of star formation could be an outer ring associated with the outer Lindblad resonance/radius of corotation. Dynamical interactions like that observed in the Cartwheel galaxy (Hernquist & Weil 1993) are probably not relevant here, as an actual merger has been produced. Resonance rings are intriguing sites of organised star formation found in some galaxies. They are probably the result of gravitational instabilities in large parts of a galaxy disk. Outer rings are usually found in barred systems (Buta & Combes 1996). When no bar is found, outer rings could be induced by a spiral mode or they could be relics formed by a dissolved bar. As pointed out above, both of the twin nuclei found in Arp 220 show barlike morphology. *N*-body simulations of resonance rings in galactic disks have been carried out by Rautiainen & Salo (2000). Their two-dimensional calculations show that outer rings are usually near the outer Lindblad resonances and that the potential outer ring region is often dominated by a slower spiral mode, which in principle could inhibit or delay ring formation.

The projected spatial distribution of young massive star clusters in Arp 220 does not behave like a monofractal with a single value for the fractal dimension. The behaviour of the projected spatial distribution of these clusters is more complex, because it cannot be characterised by a single exponent (i.e. the fractal dimension). If the super star-cluster distribution is homogeneous, D_q should not vary with q and it coincides with the Euclidean dimension. However, we find that D_q varies with q and it also appears to be a function of the time. It is a multifractal set, where a whole spectrum of singularity exponents is required in order to provide a reliable geometric description of the distribution.

Schmeja & Klessen (2006) have found that the time evolution of the clustering parameters shows that star clusters build up from several subclusters and evolves to a more centrally concentrated cluster. In principle, this trend found in young star-forming clusters in the Milky Way could be the cause of the observed decrease in the average value of the fractal dimension of the distribution of young massive star clusters in Arp 220 over time. Our results suggest that the fractal dimension declines with age, reflecting the tendency for surviving clusters to be more clumped (the inter-cluster distance increases). On the other hand, an alternative scenario for explaining a declining fractal dimension over time-scales of 500 Myr is real cluster destruction. Evolution from significant subclustering to a final state in which a few larger clusters survive decreases the number of available centres for evaluating C_q and increases the average inter-centre distance. These two factors contribute to decreasing the overall fractal dimension. Cluster destruction produces the same effects. Total cluster dissolution is mainly driven by the powerful winds of massive stars and the subsequent supernova explosions that lead to extreme mass loss leaving the cluster completely out of dynamical equilibrium (Fellhauer & Kroupa 2005). The mass of the star cluster decreases very rapidly and the characteristic velocities of the remaining stars are too high to remain bound to the dissolving cluster. This accelerates the disruption of the cluster that eventually dissolves completely. The catastrophic disruption process is even more dramatic and faster for more massive clusters, as the upper limit for the mass of the most massive stars in a cluster depends on the cluster mass (Weidner & Kroupa 2006). More massive stars imply stronger winds and earlier supernovae. This is a factor in favour of super star-cluster complexes disintegrating on a relatively short time-scale. Finally, there is even a third scenario in which the young massive star clusters evolve rapidly (within a few tens of Myr) into a significantly smaller type of star cluster, similar to the very old open clusters found in the Milky Way thick disk. This population of smaller clusters may remain undetected due to their low dynamical masses and luminosities. For young open clusters in the Milky Way (quiescent star formation) the opposite behaviour is observed with the average fractal dimension increasing over time as a result of diffusion-like processes (de la Fuente Marcos & de la Fuente Marcos 2006).

Wilson et al. (2006) state that the age segregation seen in the spatial distribution of the clusters suggests that the starburst region in Arp 220 has been decreasing over time since the merger started about 700 Myr ago (Mundell et al. 2001). The recent star formation burst near the centre appears to be the result of the collision of the remaining gas disks around each nucleus (Mundell et al. 2001). The available data appear to indicate that super star-clusters can be fully destroyed, or at least transformed into some other type of fainter star cluster, on a time-scale of a few tens of Myr. The reliability of our results depends on the quality of the positions and the completeness of the sample presented in Wilson et al. (2006). Although Wilson et al. (2006) express concern about the number of missing intermediate-age clusters at small and large radii due to the high and variable internal reddening in Arp 220, Fig. 3 shows no sign of fluctuations for $q < 0$. Large fluctuations are expected when samples are incomplete due to significant interstellar extinction. The abnormal behaviour of the multifractal spectrum for $r < 2$ kpc could be the result of incompleteness but also be connected to the presence of a supermassive binary black hole at the centre of Arp 220.

7. Conclusions

Formation of super star-clusters can be triggered during the final stages of galaxy mergers or galactic interactions, when very significant numbers of massive stars are formed out of large gas cloud systems. Giant gas cloud complexes are known to have a fractal structure due to turbulence and/or self-gravitation; therefore, super star-clusters formed out of these gas cloud complexes are expected to show a multifractal spectrum. The search for a fractal structure in galactic star-forming regions can help to identify processes that operate on a wide range of scales, such as turbulence or self-gravity. On the other hand, some galaxies exhibit dynamically-induced superstructures that overlap or even contain large-scale, star-forming regions. The fractal dimension of a set of points is an important measure of the intrinsic dimensionality of the points. In particular and after calibration, the multifractal signature (spectrum) can be used to characterise the properties of real data sets. However, when the multifractal approach is applied to an object that is dominated by one of these

superstructures (rings, shells, spiral arms), they have to be used with extreme care to avoid confusing results. The primary objective of this paper has been to calculate the fractal dimension of the distribution of young massive star clusters in Arp 220 using an empirical approach but taking the presence of any superstructure that may host the star-forming complexes into account, in our case, the ring.

The projected radial distribution of super star-clusters in Arp 220 is dominated by a prominent ring of star formation. The ring appears to extend from a radial distance of 2.0 kpc to 4.5 kpc with respect to the assumed galaxy centre. The Arp 220 annulus of star formation could be an outer ring associated with the outer Lindblad resonance/radius of corotation. After taking the presence of this annulus into account, the fractal spectrum was determined using the Minkowski-sausage method to compute the Minkowski-Bouligand dimension as a function of the parameter q. The average projected fractal dimension in the ring of star formation was found to be 1.7 ± 0.1, which is consistent with values found for non-starburst, star-forming regions in spiral galaxies. This can be interpreted as evidence in favour of the universal mechanisms responsible for global star formation with formal differences due to diverse local environmental conditions. However, the fractal dimension appears to be lower in the outer regions of the ring and, for Arp 220, this implies an actual decrease in the value of the fractal dimension over time that is probably induced by star cluster destruction. This trend is not observed under quiescent star formation.

The projected distribution of super star-clusters in Arp 220 can be described using a ring model, and it exhibits multifractal behaviour with clear signs of self-similarity. The properties of its underlying fractal geometry are similar to those found in quiescent star-forming regions in disk galaxies, although the average fractal dimension evolves differently over time by decreasing instead of increasing. This result implies that, for the short-term evolution of super cluster populations, destruction may be far more important than diffusion-like processes. This conclusion can be tested by applying the techniques described here to the distribution of young clusters in M 31 or any other galaxy with a ring of gas and star formation.

Acknowledgements. We thank Christine Wilson for providing us with electronic compilations of her data. In preparation of this paper, we made use of the NASA Astrophysics Data System and the ASTRO-PH e-print server. An anonymous referee made a number of extremely helpful suggestions which improved the paper significantly.

References

Arp, H. 1966a, Atlas of Peculiar Galaxies, California Institute of Technology, Pasadena
Arp, H. 1966b, ApJS, 14, 1
Baan, W. A., Wood, P. A. D., & Haschick, A. D. 1982, ApJ, 260, L49
Begelman, M. C., Blandford, R. D., & Rees, M. J. 1980, Nature, 287, 307
Bouligand, G. 1928a, Bull. Soc. Math. France, 52, 20
Bouligand, G. 1928b, Bull. Soc. Math. France, 52, 361
Bouligand, G. 1929, Bull. Soc. Math. France, 53, 185
Buta, R. 1986, ApJS, 61, 609
Buta, R., & Combes, F. 1996, Fund. Cosmic Phys., 17, 95
Clements, D. L., McDowell, J. C., Shaked, S., et al. 2002, ApJ, 581, 974
Elmegreen, B. G. 2002, ApJ, 577, 206
Elmegreen, B. G., & Elmegreen, D. M. 2001, AJ, 121, 1507
Elmegreen, B. G., & Falgarone, E. 1996, ApJ, 471, 816
Falconer, K. 1990, Fractal Geometry (Wiley, Chichester)
Feitzinger, J. V., & Galinski, T. 1987, A&A, 179, 249
Fellhauer, M., & Kroupa, P. 2005, ApJ, 630, 879
Freedman, W. L., Madore, B. F., Gibson, B. K., et al. 2001, ApJ, 553, 47
de la Fuente Marcos, R., & de la Fuente Marcos, C. 2006, A&A, 452, 163
Gordon, K. D., Bailin, J., Engelbracht, C. W., et al. 2006, ApJ, 638, L87
Graham, J. R., Carico, D. P., Matthews, K., et al. 1990, ApJ, 354, L5
Grassberger, P. 1983, Phys. Lett., 97A, 227
Grassberger, P., & Procaccia, I. 1983, Phys. Rev. Lett., 50, 346
Habing, H. J., et al. 1984, ApJ, 278, L59
Hearn, N. C. 2002, Ph.D. Thesis, University of Illinois at Urbana-Champaign
Hemsendorf, M., Sigurdsson, S., & Spurzem, R. 2002, ApJ, 581, 1256
Hernquist, L., & Weil, M. L. 1993, MNRAS, 261, 804
Hibbard, J. E., Vacca, W. D., & Yun, M. S. 2000, AJ, 119, 1130
Joseph, R. D., & Wright, G. S. 1985, MNRAS, 214, 87
Joseph, R. D., Wright, G. S., & Wade, R. 1984, Nature, 311, 132
Joy, M., Lester, D. F., Harvey, P. M., & Frueh, M. 1986, ApJ, 307, 110
Kroupa, P., Aarseth, S. J., & Hurley, J. 2001, MNRAS, 321, 699
Larsen, S. S., & Richtler, T. 2000, A&A, 354, 836
MacLow, M., & Klessen, R. 2004, Rev. Mod. Phys., 76, 125
Makino, J. 1997, ApJ, 478, 58
Mandelbrot, B. B. 1982, The Fractal Geometry of Nature (San Francisco: W. H. Freeman)
Mandelbrot, B. B. 1985, Phys. Scr., 32, 257
Minkowski, H. 1900, Jahresber. Deutsch. Math.-Verein., 9, 115
Mundell, C. G., Ferruit, P., & Pedlar, A. 2001, ApJ, 560, 168
Nilson, P. 1973, Uppsala General Catalogue of Galaxies, Uppsala Astr. Obs. Ann., v. 6
Norris, R. P. 1985, MNRAS, 216, 701
Norris, R. P., Baan, W. A., Haschick, A. D., Diamond, P. J., & Booth, R. S. 1984, MNRAS, 213, 821
Paladin, G., & Vulpiani, A. 1987, Phys. Rep., 156, 147
Rice, W. 1993, AJ, 105, 67
Rieke, G. H., Cutri, R. M., Black, J. H., et al. 1985, ApJ, 290, 116
Rautiainen, P., & Salo, H. 2000, A&A, 362, 465
Sakamoto, K., Scoville, N. Z., Yun, M. S., et al. 1999, ApJ, 514, 68
Sánchez, N., Alfaro, E. J., & Pérez, E. 2005, ApJ, 625, 849
Sanders, D. B., Soifer, B. T., Elias, J. H., et al. 1988, ApJ, 325, 74
Sanders, D. B., Mazzarella, J. M., Kim, D.-C., Surace, J. A., & Soifer, B. T. 2003, AJ, 126, 1607
Schmeja, S., & Klessen, R. S. 2006, A&A, 449, 151
Schroeder, M. 1991, Fractals, Chaos, Power Laws: Minutes from an Infinite Paradise (New York: W. H. Freeman & Co.)
Scoville, N. Z., Evans, A. S., Dinshaw, N., et al. 1998, ApJ, 492, L107
Shaya, E., Dowling, D. M., Currie, D. G., Faber, S. M., & Groth, E. J. 1994, AJ, 107, 1675
Shioya, Y., Taniguchi, Y., & Trentham, N. 2001a, MNRAS, 321, 11
Shioya, Y., Trentham, N., & Taniguchi, Y. 2001b, ApJ, 548, L29
Soifer, B. T., Neugebauer, G., Helou, G., et al. 1984, ApJ, 283, L1
Soifer, B. T., Neugebauer, G., Matthews, K., et al. 1999, ApJ, 513, 207
Spoon, H. W. W., Moorwood, A. F. M., Lutz, D., et al. 2004, A&A, 414, 873
Stocke, J. T., Tifft, W. A., & Kaftan-Kissim, M. A. 1978, ApJ, 83, 322
Tilley, D. A., & Pudritz, R. E. 2004, MNRAS, 353, 769
de Vaucouleurs, G., de Vaucouleurs, A., Corwin, H. G., et al. 1991, Third Reference Catalogue of Bright Galaxies (Berlin: Springer)
Weedman, D. W., Feldman, F. R., Balzano, V. A., et al. 1981, ApJ, 248, 105
Weidner, C., & Kroupa, P. 2006, MNRAS, 365, 1333
Whitmore, B. C., Zhang, Q., Leitherer, C., et al. 1999, AJ, 118, 1551
Wilson, C. D., Harris, W. E., Longden, R., & Scoville, N. Z. 2006, ApJ, 641, 763
Wu, K. K. S., Alexander, P., & Sleath, J. P. 1997, MNRAS, 286, 777
Yadav, J., Bharadwaj, S., Pandey, B., & Seshadri, T. R. 2005, MNRAS, 364, 601